Eur. J. Mineral., 38, 325–336, 2026
https://doi.org/10.5194/ejm-38-325-2026

European Journal of Mineralogy
Open Access

Argentotennantite-(Fe), $Ag_6(Cu_4Fe_2)As_4S_{13}$, a new member of the tetrahedrite group from the San Genaro mine, Peru: occurrence and crystal structure

Jiří Sejkora[1,2], Dalibor Velebil[1], Cristian Biagioni[3,4], Zdeněk Dolníček[1], and Jaroslav Hyršl[5]

[1]Department of Mineralogy and Petrology, National Museum, Cirkusová 1740, 193 00, Praha 9, Czech Republic
[2]Earth Sciences Institute, v.v.i., Slovak Academy of Sciences, Dúbravská cesta 9, 840 05 Bratislava, Slovakia
[3]Dipartimento di Scienze della Terra, Università di Pisa, Via Santa Maria, 53, 56126 Pisa, Italy
[4]Centro per l'Integrazione della Strumentazione scientifica dell'Università di Pisa (CISUP), Università di Pisa, Pisa, Italy
[5]Ke kurtům 383, 142 00 Praha 4, Czech Republic

Correspondence: Jiří Sejkora (jiri.sejkora@nm.cz)

Received: 27 April 2026 – Revised: 16 May 2026 – Accepted: 20 May 2026 – Published: 11 June 2026

Abstract. Argentotennantite-(Fe), $Ag_6(Cu_4Fe_2)As_4S_{13}$, has been approved as a new mineral species (IMA 2023-126) by the Commission on New Minerals, Nomenclature and Classification of the International Mineralogical Association (CNMNC-IMA) using a sample of quartz gangue with argentotetrahedrite-(Zn), pyrargyrite, baryte, and siderite from the San Genaro mine, Castrovirreyna Province, Huancavelica, Peru. Argentotennantite-(Fe) occurs as anhedral grains up to 100 µm in size. More commonly, it forms micrometer-sized rims around crystals of argentotetrahedrite-(Zn) or replaces the latter around cavities and fissures, along with Ag-rich tennantite-(Fe). Argentotennantite-(Fe) is opaque and dark gray in color, with a metallic luster and black streak. In reflected light, it is isotropic and pale gray, with a brownish shade. The reflectance values for wavelengths recommended by the Commission on Ore Mineralogy of the IMA, measured in air, are as follows [λ (nm, R (%)]: 470, 29.9; 546, 30.1; 589, 29.8; and 650, 28.9. The chemical formula of the grain used for the crystal structure study, recalculated on the basis of $\Sigma Me = 16$ atoms per formula unit, is $(Ag_{3.36}Cu_{2.70})_{\Sigma 6.06}(Cu_{4.05}Fe_{1.88}Zn_{0.07})_{\Sigma 6.00}(As_{2.29}Sb_{1.66})_{\Sigma 3.95}S_{12.82}$. Argentotennantite-(Fe) is cubic, $I\bar{4}3m$, with $a = 10.4365(5)$ Å, $V = 1136.75(17)$ Å^3, and $Z = 2$. Its crystal structure has been refined by single-crystal X-ray diffraction data to a final $R_1 = 0.0384$ on the basis of 246 unique reflections with $F > 4\sigma_F$ and 20 refined parameters. Argentotennantite-(Fe) is isotypic with other members of the tetrahedrite group. Structural relationships between argentotennantite-(Fe) and selected members of the tetrahedrite-group minerals are discussed, and previous findings relating to this species are briefly reviewed.

1 Introduction

Tetrahedrite-group minerals (TGMs) are the most common sulfosalts in many hydrothermal ore deposits. These chalcogenides form a complex isotypic series, with the general structural formula $^{M(2)}A_6^{M(1)}(B_4C_2)^{X(3)}D_4^{S(1)}Y_{12}^{S(2)}Z$, where A = Cu^+, Ag^+, □ (vacancy), or they can be represented by an $(Ag_6)^{4+}$ cluster; B = Cu^+ and Ag^+; C = Zn^{2+}, Fe^{2+}, Hg^{2+}, Cd^{2+}, Ni^{2+}, Mn^{2+}, Cu^{2+}, Cu^+, In^{3+}, and Fe^{3+}; D = Sb^{3+}, As^{3+}, Bi^{3+}, and Te^{4+}; Y = S^{2-} and Se^{2-}; and Z = S^{2-}, Se^{2-}, and □ (Biagioni et al., 2020). Thus, tetrahedrite-group minerals are characterized by different homovalent and heterovalent substitutions and represent an interesting link between mineralogy and ore geochemistry. This wide chemical variability, often observed across a deposit or individual veins, has been used by some authors to

constrain ore-forming processes (e.g., Kovalenker and Bortnikov, 1985; Staude et al., 2010; Kemkin and Kemkina, 2013; Wei et al., 2021; Šoster et al., 2024; Pažout et al., 2026; Biagioni et al., 2026).

Even if TGMs are one of the main Ag carriers in ore deposits, due to their widespread occurrence, they also represent an environmental risk under weathering conditions, being the source of potentially toxic elements (e.g., Sb, As, Cu, Cd, Hg; Keith and Telliard, 1979). Recently, some authors studied the associations of supergene minerals derived from TGM alteration, giving some insights into the mobility of these toxic elements in different geological environments (e.g., Borčinová Radková et al., 2017; Keim et al., 2018; Majzlan et al., 2018; D'Orazio et al., 2024). Moreover, TGMs are also currently being actively studied for their high-tech, especially thermoelectric, properties (e.g., Chetty et al., 2015; Weller and Morelli, 2022; Rout et al., 2023; Sun et al., 2024).

The classification and nomenclature of the TGMs, in keeping with the current IMA-accepted rules, were published by Biagioni et al. (2020). Following this revision of the nomenclature of TGMs, a renewed interest in these common sulfosalts, occurring in different kinds of hydrothermal ore deposits, has allowed the identification of several new mineral species and the collection of high-quality crystal chemical data. Since the publication of this nomenclature, 28 new mineral species have been characterized (https://www.mindat.org/min-29338.html, last access: 16 May 2026), emphasizing the chemical variability of this isotypic group.

Silver-rich members with 3 to 6 Ag atoms per formula unit (apfu) (A-constituent, freibergite/arsenofreibergite series) have been known for a long time. Indeed, freibergite was first described from the Hab Acht Mine near Freiberg, Saxony (Germany), by von Weissenbach (1831) and was named by Kenngott (1853). Currently IMA-accepted mineral species belonging to the freibergite series are argentotetrahedrite-(Fe) (Welch et al., 2018), argentotetrahedrite-(Hg) (Wu et al., 2022), argentotetrahedrite-(Zn) (Sejkora et al., 2022), argentotetrahedrite-(Cd) (Mikuš et al., 2023), kenoargentotetrahedrite-(Fe) (the former freibergite – Welch et al., 2018; Biagioni et al., 2020), and kenoargentotetrahedrite-(Zn) (Qu et al., 2024). The arsenofreibergite series comprises fewer and rarer species, being currently represented only by argentotennantite-(Zn) (Spiridonov et al., 1986; Biagioni et al., 2020) and kenoargentotennantite-(Fe) (Biagioni et al., 2026). The occurrence of the new species argentotennantite-(Fe) in a sample from the San Genaro mine (Peru) was mentioned by Velebil et al. (2021) on the basis of electron microprobe data.

The new detailed study of the chemical composition of this sample of argentotennantite-(Fe) and the refinement of its crystal structure allowed the submission of a formal proposal to the IMA-CNMNC, and, subsequently, the mineral and its name (symbol Atnt-Fe) were approved (IMA 2023-126).

Figure 1. Central part of the San Genaro mine in 2005. Photo: Jaroslav Hyršl.

Holotype material (polished section) of argentotennantite-(Fe) is deposited in the collections of the Department of Mineralogy and Petrology, National Museum in Prague, Cirkusová 1740, 19300 Praha 9, Czech Republic, under the catalogue number P1P 52/2023. The crystal used for the single-crystal X-ray diffraction study is kept in the mineralogical collection of the Museo di Storia Naturale of the Università di Pisa, Via Roma 79, Calci (PI), under catalogue number 20070.

2 Occurrence and physical properties

Argentotennantite-(Fe) was found in a sample from the central part of the San Genaro mine (GPS 13°11′37″ S, 75°08′57″ W), Castrovirreyna Province, Huancavelica, Peru. The San Genaro mine (Fig. 1) is located in the eastern part of the Castrovirreyna mining district, north of the Laguna Orcococha at elevations between 4750 and 5000 m a.s.l. This ore district was discovered in 1591 and had many periods of intermittent operation. There is no recent ore production at the San Genaro area, but the mine is scheduled to be reopened in future.

The San Genaro mine exploited hydrothermal veins rich in silver sulfosalts (with lengths of up to 2.5 km and thicknesses of about 1 m), which struck more or less E–W within the late Miocene (11–12 Ma) andesite to rhyolite rocks. Hydrothermal mineralization is accompanied by argillic and propylitic alteration. The main ore minerals are galena, sphalerite, enargite, acanthite, polybasite- and tetrahedrite-group minerals, chalcopyrite, and pyrargyrite; the gangue minerals are quartz and pyrite, with minor baryte, calcite, rhodochrosite, siderite, and hematite. The geological background of the San Genaro mine has been described in Lewis (1964), Crowley et al. (1997), Wise (2005), and Hyršl et al. (2010). It is the type locality of two other sulfosalt species: baumstarkite (Effenberger et al., 2002) and sangenaroite (Topa et al., 2019).

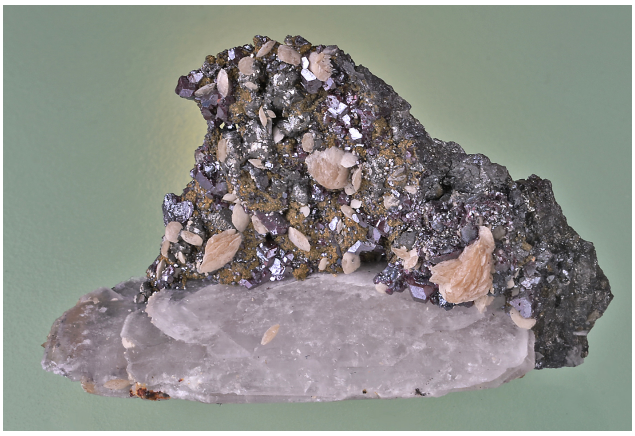

Figure 2. Abundant dark-red pyrargyrite and dark-gray TGM crystals, formed by predominant argentotetrahedrite-(Zn) with rims of argentotennantite-(Fe) to Ag-rich tennantite-(Fe). Associated minerals are also minor galena and acanthite on quartz gangue with light-pink siderite crystals and large white tabular baryte crystals in the bottom part of the sample; San Genaro mine, Peru. Sample size: 4.3 cm. Collection of Jaroslav Hyršl, Prague (no. 4.3-17). Photo: Jaroslav Hyršl.

Argentotennantite-(Fe) has been identified as part of a specimen (Fig. 2) represented by quartz gangue with abundant dark-red pyrargyrite (up to 3 mm) and dark-gray TGM multi-faced crystals (predominantly argentotetrahedrite-(Zn) with rims of argentotennantite-(Fe) to Ag-rich tennantite-(Fe)) up to 2 mm in size, with minor galena, acanthite, and light-pink siderite and white tabular baryte crystals. Argentotennantite-(Fe) occurs as anhedral grains up to 100 µm in size (Fig. 3), but more commonly it forms micrometer-sized rims around crystals of argentotetrahedrite-(Zn) (Fig. 4a) or replaces the latter around cavities (Fig. 4b) and fissures (Fig. 4c), along with Ag-rich tennantite-(Fe).

It is opaque and dark gray in color, with a black streak. The luster is metallic. The Mohs hardness may be close to 4, in agreement with other members of the tetrahedrite group. Argentotennantite-(Fe) is brittle, with an indistinct cleavage and a conchoidal fracture. Density was not measured, owing to the small amount of available material; on the basis of the empirical formula and the single-crystal unit-cell parameters, the calculated density is 4.922 g cm^{-3}. In reflected light, argentotennantite-(Fe) is isotropic. It is pale gray, with a brownish shade. Internal reflections were not observed. Reflectance values, measured in air using a spectrophotometer MSP400 Tidas at Leica microscope, with a 50× objective, are given in Table 1 and shown in Fig. 5, where they are compared with published data for kenoargentotennantite-(Fe) and tennantite-(Fe).

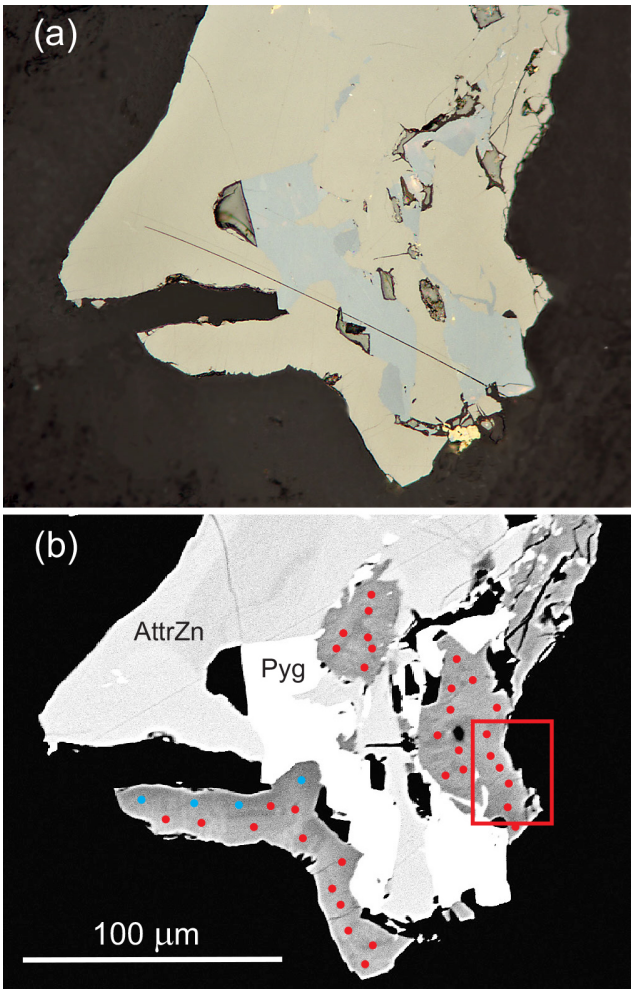

Figure 3. Reflected light **(a)** and backscattered electron **(b)** images of the holotype sample. In **(b)**, argentotennantite-(Fe) corresponds to the red circles, whereas blue circles correspond to Ag-rich tennantite-(Fe). Light gray is argentotetrahedrite-(Zn) (AttrZn), whereas white is pyrargyrite (Pyg). The grain used from the single-crystal X-ray diffraction study was extracted from the red box.

3 Experimental

3.1 Chemical analyses

Quantitative chemical analyses were carried out using a Cameca SX100 electron microprobe at the National Museum of Prague (Czech Republic). Experimental conditions were as follows: WDS mode, accelerating voltage of 25 kV, beam current of 20 nA, and beam diameter of 0.7 µm. Standards (element, emission line) were as follows: Ag metal (Ag$L\alpha$), Bi_2Se_3 (Bi$M\beta$), CdTe (Cd$L\alpha$), chalcopyrite (Cu$K\alpha$, S$K\alpha$), pyrite (Fe$K\alpha$), PbS (Pb$M\alpha$), NiAs (As$L\beta$), Sb_2S_3 (Sb$L\alpha$), Tl(Br,I) (Tl$L\alpha$), and ZnS (Zn$K\alpha$). The peak counting times were 20 s for all elements, and 10 s for each background. Other elements (i.e., Au, Cl, Co, Ga, Ge, Hg, In, Mn, Ni,

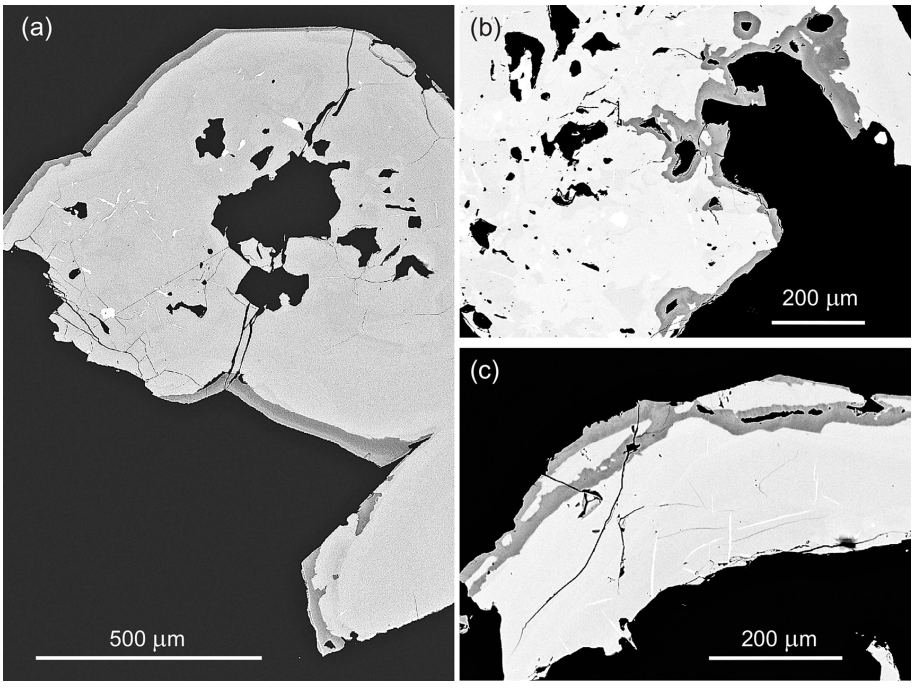

Figure 4. Backscattered electron images of the rims of argentotennantite-(Fe) to Ag-rich tennantite-(Fe) (dark gray) **(a)** around crystals of argentotetrahedrite-(Zn), **(b)** around the surface and cavities of argentotetrahedrite-(Zn), and **(c)** around fissures in argentotetrahedrite-(Zn). Argentotetrahedrite-(Zn) (light gray) usually contains tiny inclusions of pyrargyrite (white).

Table 1. Reflectance data for argentotennantite-(Fe)*.

λ (nm)	*R* (%)	λ (nm)	*R* (%)
400	30.3	560	30.0
420	30.2	580	29.9
440	30.1	**589**	**29.8**
460	29.9	600	29.7
470	**29.9**	620	29.5
480	30.0	640	29.2
500	30.1	**650**	**28.9**
520	30.2	660	28.8
540	30.1	680	28.6
546	**30.1**	700	28.3

* The reference wavelengths required by the Commission on Ore Mineralogy (COM) are given in bold.

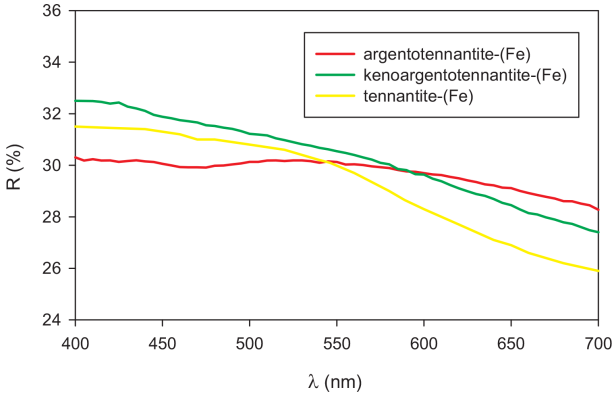

Figure 5. Comparison of the reflectance curves of Fe-dominant members of the tennantite and arsenofreibergite series; argentotennantite-(Fe) from the San Genaro mine, Peru (this paper); kenoargentotennantite-(Fe) from the Pollone mine, Valdicastello Carducci, Italy (Biagioni et al., 2026); tennantite-(Fe), Wheal Jewel, Gwennap, Cornwall, UK (Criddle and Stanley, 1993).

Sn, Se, and Te) were found to be below the detection limits (0.02 wt %–0.10 wt %). Matrix correction by PAP procedure (Pouchou and Pichoir, 1985) was applied to the data. As reported in other papers (e.g., Biagioni et al., 2020; Sejkora et al., 2021), there are several different approaches to calculate the chemical formula of the TGMs. Due to possible vacancies at the S(2) site in the Ag-rich members, the best approaches are as follows: (1) normalization on the basis of $\Sigma Me = 16$ apfu, assuming that no vacancies occur at $M(2)$, $M(1)$, and $X(3)$, or (2) normalization on the basis of $(As + Sb) = 4$ apfu, taking into account that previous studies (e.g., Johnson et al., 1986) revealed that negligible variations with respect to the ideal number of $X(3)$ atoms occur. The results of our study indicate that only very minor vacancies, if any, possibly occur at $M(2)$, $M(1)$, and $X(3)$ sites, and, therefore, the first approach was selected for calculation. Chemical data for the grain of argentotennantite-(Fe) used for the single-crystal X-ray diffraction study are given in Table 2,

Table 2. Chemical data for argentotennantite-(Fe) (holotype sample – grain used for single crystal study).

Element	Mean	Range	E.s.d.
Cu	25.34	24.98–26.25	0.52
Ag	21.38	20.65–21.78	0.45
Fe	6.20	6.08–6.29	0.08
Zn	0.27	0.23–0.29	0.03
As	10.12	9.24–11.99	1.11
Sb	11.90	9.31–13.20	1.53
S	24.28	24.07–24.75	0.27
Total	99.49	99.22–99.65	0.16

Mean and range of five spot analyses; e.s.d. denotes estimated standard deviation.

whereas Table S1 in the Supplement reports the full dataset (386 spot analyses in total) of the chemical analyses of the described TGMs.

3.2 X-ray crystallography

A single-crystal X-ray diffraction study of argentotennantite-(Fe) was performed on a small grain ($0.035 \times 0.030 \times 0.025$ mm) extracted from the rim of an aggregate of pyrargyrite and argentotetrahedrite-(Zn) (Fig. 3). Data collection was performed using a Bruker D8 Venture four-circle diffractometer equipped with an air-cooled Photon III detector and microfocus Mo$K\alpha$ radiation (Centro per l'Integrazione della Strumentazione scientifica dell'Università di Pisa, University of Pisa, Italy). The detector-to-crystal distance was set to 38 mm. Data were collected using φ scan modes, in 0.5° slices, with an exposure time of 20 s per frame. A total of 216 frames were collected, and they were integrated with the Bruker SAINT software package using a narrow-frame algorithm. Data were corrected for Lorentz polarization, absorption, and background. Unit-cell parameters were refined on the basis of the XYZ centroids of 498 reflections above $20\ \sigma I$ with $5.52 < 2\theta < 56.30°$ as $a = 10.4365(5)$ Å, and $V = 1136.75(17)$ Å^3, with space group $I\bar{4}3m$.

The crystal structure of argentotennantite-(Fe) was refined using Shelxl-2018 (Sheldrick, 2015) starting from the atomic coordinates of Johnson and Burnham (1985). The occurrence of the racemic twin was modeled, and the structure had to be inverted. The following neutral scattering curves, taken from the International Tables for Crystallography (Wilson, 1992), were used: Cu vs. Ag at the $M(2)$ site, Cu vs. Fe at $M(1)$, As vs. Sb at $X(3)$, and S at the S(1) and S(2) sites. The scattering factors of Cu (Z = 29) and Fe (Z = 26) are similar, and, consequently, the site occupancy at $M(1)$ was fixed on the basis of electron microprobe data, idealizing the occupancy at ($Cu_{0.67}Fe_{0.33}$). After several cycles of isotropic refinement, the R_1 converged to 0.0842, confirming the correctness of the structural model. The anisotropic model for both cations and anions converged to $R_1 = 0.0384$ for 246 reflections with $F > 4\sigma_F$ and 20 refined parameters. The details of data collection and refinement are given in Table 3. Fractional atom coordinates and equivalent isotropic displacement parameters are reported in Table 4. Table 5 reports selected bond distances, whereas weighted bond-valence sums, calculated according to Brese and O'Keeffe (1991), are shown in Table 6. The crystallographic information files (CIFs) are deposited in the Supplement of this paper.

Powder X-ray diffraction data could not be collected due to the paucity of available material. Consequently, powder X-ray diffraction data, given in Table 7, were calculated through the software PowderCell 2.3 (Kraus and Nolze, 1996) using the structural model of argentotennantite-(Fe) discussed below.

4 Results and discussion

4.1 Chemical data for argentotennantite-(Fe) and associated tetrahedrite-group minerals

Chemical data for the holotype grain of argentotennantite-(Fe) used for the single-crystal X-ray diffraction study are given in Table 2 and correspond to the following formula: $Ag_{3.36(9)}Cu_{6.75(9)}Fe_{1.88(2)}Zn_{0.07(1)}As_{2.29(23)}Sb_{1.66(22)}S_{12.82(5)}$. Taking into account the results of the crystal structure refinement (see below), the crystal chemical formula can be written as $^{M(2)}(Ag_{3.36}Cu_{2.70})_{\Sigma 6.06}\ ^{M(1)}(Cu_{4.05}Fe_{1.88}Zn_{0.07})_{\Sigma 6.00}\ ^{X(3)}(As_{2.29}Sb_{1.66})_{\Sigma 3.95}^{S(1)+S(2)}S_{12.82}$. The end-member formula of argentotennantite-(Fe) is $Ag_6(Cu_4Fe_2)As_4S_{13}$ ($Z = 2$), corresponding to (in wt %) Cu 14.70, Ag 37.42, Fe 6.46, As 17.33, S 24.10, and total 100.00.

The chemical compositions for other argentotennantite-(Fe) grains and for associated Ag-rich tennantite-(Fe) and argentotetrahedrite-(Zn) are given in Table S1. Late-stage rims of TGM crystals (Figs. 3 and 4) are represented by zoned argentotennantite-(Fe) to Ag-rich tennantite-(Fe), with a negative correlation between Ag and As (Fig. 6b) and a less distinct negative correlation of Ag and S contents (Fig. 6c). All compositions belong to Fe- and As-dominant members with S contents > 12.5 apfu (Fig. 6a–c). The silver contents of argentotennantite-(Fe) are found to lie in the range of 3.00–3.68 apfu; the mineral is Fe-dominant (1.64–1.93 apfu), with only minor Zn (up to 0.25 apfu) and traces of Cu^{2+}, Pb, and Cd of up to 0.08, 0.04, and 0.01 apfu, respectively. Arsenic (1.98–3.25 apfu) is partly substituted by Sb (0.69–1.97 apfu), and S contents were found to be in the range 12.54–13.07 apfu. For Ag-rich tennantite-(Fe), Ag contents are in the range of 2.23–2.99 apfu; it is Fe-dominant (1.30–1.95 apfu), with minor Zn (up to 0.60 apfu) and, locally, traces of Pb and Cd of up to 0.04 and 0.01 apfu, respectively. The calculated Cu^{2+} contents occasionally reach up to 0.27 apfu but are usually only around 0.05 apfu. The dominant As (2.66–3.82 apfu) is accompanied by Sb (0.11–1.22 apfu), and S contents were determined to be in the range 12.61–13.18 apfu.

Table 3. Crystal and experimental data for argentotennantite-(Fe).

Crystal data	
Crystal size (mm)	$0.035 \times 0.030 \times 0.025$
Cell setting, space group	Cubic, $I\bar{4}3m$
a (Å)	10.4365(5)
V (Å^3)	1136.75(17)
Z	2
Data collection and refinement	
Radiation, wavelength (Å)	Mo$K\alpha$, $\lambda = 0.71073$
Temperature (K)	293(2)
$2\theta_{max}$ (°)	56.30
Measured reflections	2145
Unique reflections	284
Reflections with $F > 4\sigma_F$	246
R_{int}	0.0614
$R\sigma$	0.0507
Range of h, k, l	$-9 \le h \le 13$, $-12 \le k \le 13$, $-13 \le l \le 13$
R [$F > 4\sigma_F$]	0.0384
R (all data)	0.0476
wR (on F^2)[a]	0.0984
Goof	1.162
Absolute structure parameter[b]	−0.04(13)
Number of least-squares parameters	20
Maximum and minimum residual peak (e Å^{-3})	1.34 [at 1.07 Å from $M(2)$] −1.18 [at 0.83 Å from $M(2)$]

[a] $w = 1/[\sigma^2(F_o^2)+(0.0001P)^2+31.5623P]$. [b] Flack (1983).

Table 4. Site, site occupancy (s.o.), fractional atom coordinates, and equivalent isotropic displacement parameters (Å^2) for argentotennantite-(Fe).

Site	S.o.	x/a	y/b	z/c	U_{eq}
$M(2)$	$Ag_{0.53(4)}Cu_{0.47(4)}$	0.7852(5)	0	0	0.076(2)
$M(1)$	$Cu_{0.67}Fe_{0.33}$	3/4	1/2	0	0.0211(12)
$X(3)$	$As_{0.53(3)}Sb_{0.47(3)}$	0.73447(13)	0.73447(13)	0.73447(13)	0.0174(7)
S(1)	$S_{1.00}$	0.8769(3)	0.8769(3)	0.6361(4)	0.0159(9)
S(2)	$S_{1.00}$	0	0	0	0.123(14)

Table 5. Selected bond distances (in Å) for argentotennantite-(Fe).

$M(1)$	– S(1) ×4	2.328(3)
$M(2)$	– S(2)	2.242(6)
	– S(1) ×2	2.392(5)
$X(3)$	– S(1) ×3	2.340(5)

The relatively uniform chemical composition of early-stage TGM crystals (Figs. 3 and 4) is significantly different (Fig. 6) and corresponds to argentotetrahedrite-(Zn) (Sejkora et al., 2022), with 3.21–3.29 apfu Ag as the A-chemical constituent. The dominant Me^{2+} element is Zn (1.46–1.92 apfu), accompanied by minor Fe (0.02–0.43 apfu) and Cd (0.02–0.05 apfu); calculated Cu^{2+} contents are low (up to 0.09 apfu). The extent of $AsSb_{-1}$ substitution is limited to 0.60 apfu As, and contents of S (12.76–13.16 apfu) are close to the ideal value of 13 apfu. The average formula (28 spot analyses) can be expressed as $(Ag_{3.25}Cu_{2.73})_{\Sigma 5.98}[Cu_{4.00}(Zn_{1.73}Fe_{0.19}Cu_{0.04}Cd_{0.04})_{\Sigma 2.00}]_{\Sigma 6.00}(Sb_{3.76}As_{0.26})_{\Sigma 4.02}S_{13.02}$.

4.2 Crystal structure description

The crystal structure of argentotennantite-(Fe) agrees with the general features of the members of the tetrahedrite isotypic group, i.e., a collapsed sodalite-like framework formed by corner-sharing $M(1)S(1)_4$ tetrahedra with cages

Table 6. Weighted bond-valence sums (in valence units) in argentotennantite-(Fe).

Site	$M(1)$	$M(2)$	$X(3)$	Σanions	Theor.
S(1)	$^{2\times\rightarrow}0.40^{\times4\downarrow}$	$0.39^{\times2\downarrow}$	$1.06^{\times3\downarrow}$	2.25	2.00
S(2)		$^{6\times\rightarrow}0.58$		3.48	2.00
Σcations	1.60	1.36	3.18		
Theor.	1.33	1.00	3.00		

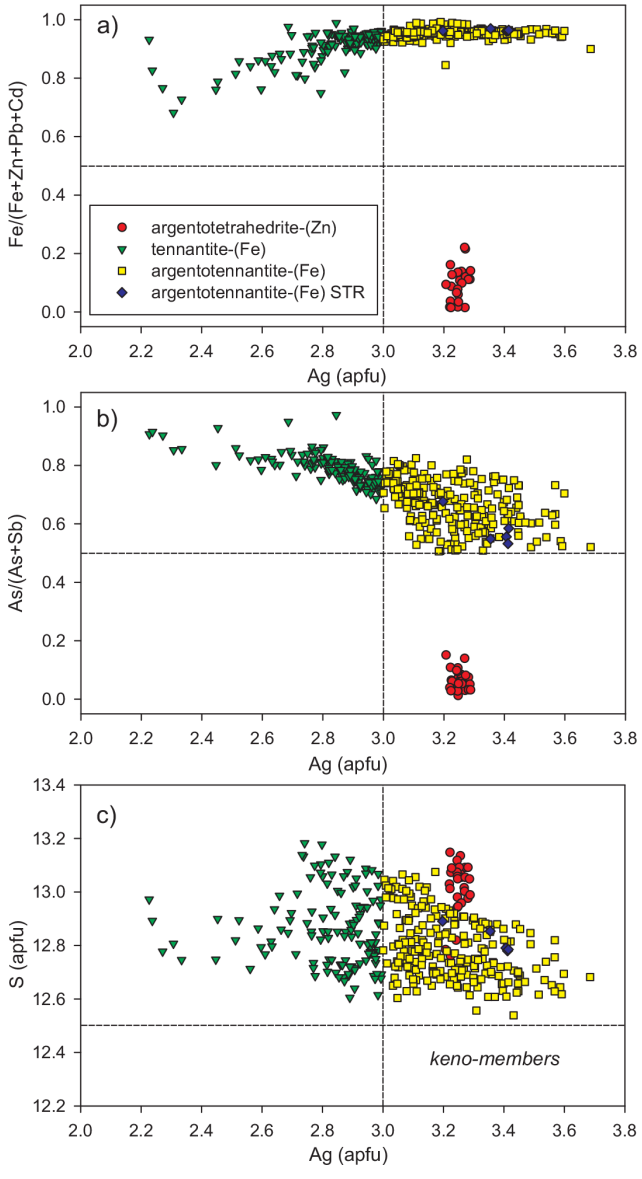

Figure 6. Chemical relationships (in apfu) between Ag vs. Fe / (Fe + Zn + Pb + Cd) **(a)**, Ag vs. As / (As + Sb) **(b)**, Zn vs. Fe **(c)**, and Ag vs. S **(d)** in studied tetrahedrite-group minerals from San Genaro. STR – data of fragment used for the crystal structure study.

Table 7. Calculated X-ray powder diffraction data for argentotennantite-(Fe). Intensity and d_{hkl} were calculated using the software PowderCell 2.4 (Kraus and Nolze, 1996) on the basis of the structural model given in Table 4. Only reflections with $I_{calc} > 1$ are listed. The five strongest reflections are given in bold.

I_{calc}	d_{calc}	$h\ k\ l$
9	**7.380**	**1 1 0**
2	4.261	2 1 1
3	3.690	2 2 0
1	3.300	3 1 0
100	**3.013**	**2 2 2**
5	2.789	3 2 1
20	**2.609**	**4 0 0**
2	2.460	3 3 0
5	2.460	4 1 1
1	2.334	4 2 0
3	2.225	3 3 2
3	2.047	5 1 0
5	2.047	4 3 1
5	1.905	5 2 1
39	**1.845**	**4 4 0**
1	1.790	4 3 3
1	1.739	4 4 2
4	1.693	6 1 1
1	1.693	5 3 2
1	1.650	6 2 0
1	1.610	5 4 1
21	**1.573**	**6 2 2**
1	1.539	6 3 1
2	1.506	4 4 4
1	1.476	7 1 0
1	1.476	5 4 3
1	1.476	5 5 0

hosting S(2)-centered $M(2)$-octahedra, surrounded by four $X(3)S(1)_3$ trigonal pyramids (e.g., Johnson et al., 1988).

The $M(2)$ site shows a planar triangular coordination, with an average $\langle M(2)\text{–S}\rangle$ distance of 2.342 Å. The refinement of its site occupancy points to $Ag_{0.53(4)}Cu_{0.47(4)}$, corresponding to a mean atomic number (MAN) of 38.54 electrons, to be compared with the value obtained during electron microprobe analyses, i.e., ∼ 39 electrons (38.99 normalizing the sum of Ag and Cu to one atom at the $M(2)$ site). In other isotypic Ag members of the tetrahedrite group, e.g., argentotetrahedrite-(Zn) (Sejkora et al.,

2022) and zvěstovite-(Zn) (Sejkora et al., 2021), the $M(2)$ site was found to be split. It is very probable that, in argentotennantite-(Fe), such a splitting also occurs, as testified to by the high U_{eq} value observed at this site, i.e., 0.076(2) Å^2, as well as the high residuals around the $M(2)$ site and the $M(2)$–S distances, physically too short when the site is occupied by Ag. A split model suggests the preferential occupancy of Cu at $M(2a)$ and Ag at $M(2b)$, as supported by observed average bond distances. However, some correlations higher than 0.8 were found during the refinement of the split model, and consequently an unsplit model is presented. The bond-valence sum is 1.36 valence units (v.u.).

The tetrahedrally coordinated $M(1)$ site has an average $\langle M(1)\text{–S}\rangle$ bond distance of 2.329 Å. Electron microprobe analysis agrees with an ideal $(Cu_{0.67}Fe_{0.33})$ site occupancy, with a minor replacement of these elements by Zn. On the basis of this proposed site occupancy, the bond-valence sum at the $M(1)$ site is 1.60 *v.u.*, larger than the theoretical value of 1.33 *v.u.*

The $X(3)$ site is a mixed (As, Sb) position, with an average $\langle X(3)\text{–S}\rangle$ distance of 2.340 Å. Considering the ideal As–S and Sb–S distances of 2.26 and 2.45 Å, respectively, calculated on the basis of the bond parameters of Brese and O'Keeffe (1991), the observed average distance should correspond to the site occupancy $(As_{0.58}Sb_{0.42})$, to be compared with the results of crystal structure refinement $(As_{0.53}Sb_{0.47})$ and electron microprobe analysis $(As_{0.58}Sb_{0.42})$. The bond-valence sum, calculated on the basis of the refined site occupancy, is 3.18 *v.u.*

The S(1) and S(2) sites are fully occupied by S. The S(2)-centered octahedron has a volume of ∼ 15 Å^3, in accord with an S(2)$M(2)_6$-occupied octahedron (e.g., Welch et al., 2018; Sejkora et al., 2022; Biagioni et al., 2026). The bond-valence sums of S atoms at S(1) and S(2) are 2.25 and 3.48 *v.u.*, respectively. Both S atoms are overbonded, mainly due to the too-short Ag–S distances. This is particularly true for the S atom hosted at the S(2) position, resulting in an exceptionally high overbonding. This feature has been observed in all of the other known Ag members of the tetrahedrite group, e.g., in argentotetrahedrite-(Zn) (bond-valence sums ranging between 3.00 and 3.30 *v.u.* for the three refined samples), zvěstovite-(Zn) (3.24 *v.u.*), and zvěstovite-(Fe) (2.76 *v.u.*) (Sejkora et al., 2021, 2022; Biagioni et al., 2024). This is due to the short $M(2)$–S(2) bond distance, definitely shorter than the ideal $\langle^{[III]}\text{Ag–S}\rangle$ distance, i.e., 2.56 Å. The physically unrealistic distances may be due to some disorder affecting both the S(2) position (e.g., Sejkora et al., 2022) and the $M(2)$ site. The former shows a high U_{eq} value (0.12 Å). A high value of U_{eq} could be related to a positional disorder or to an incorrect refinement of the site occupancy at S(2). As no significant vacancies are suggested by the chemical analyses, by the refinement of its site occupancy (pointing to a full occupancy), or by the volume of the S(2)-centered octahedron, the former hypothesis is more probable. This could be in accord with Peterson and Miller (1986), who proposed that, in order to achieve longer Ag–S distances, S(2) should be displaced from the 2*a* position. Indeed, as in argentotetrahedrite-(Fe), in argentotennantite-(Fe), a residual at the 8*c* (x, x, x) position, with $x = 0.0448$, was also observed in the difference-Fourier map. Moreover, as discussed above, the U_{eq} value at the $M(2)$ site is high and also suggests a splitting of this position into at least two sub-sites able to achieve physically sound bond distances (e.g., Biagioni et al., 2024).

The structural formula of argentotennantite-(Fe), based on electron microprobe data and crystal structure refinement, could be written as $^{M(2)}(Ag_{3.18}Cu_{2.82})^{M(1)}_{\Sigma 6.00}(Cu_{4.00}Fe_{2.00})^{X(3)}_{\Sigma 6.00}(As_{2.12}Sb_{1.88})^{S(1)+S(2)}_{\Sigma 4.00}S_{13}$ $(Z = 2)$.

Johnson et al. (1987) proposed the following relation between the unit-cell parameter a and the chemistry of the studied sample: a (Å) $= 10.379 + 0.082(\text{Ag}) - 0.01(\text{Ag}^2) - 0.009(\text{Cu}^*) + 0.066(\text{Hg}) - 0.038(\text{As}) + 0.144(\text{Bi})$. On the basis of the formula derived from the structural analysis, the calculated unit-cell parameter is $a = 10.46$ Å, which aligns with the observed value of 10.44 Å.

4.3 Crystal chemical features of arsenofreibergite-series minerals and the role of Sb in their stability

The name "arsenofreibergite" was introduced by Biagioni et al. (2020) as a series name to indicate the As analogues of the freibergite-series minerals. At that time, only argentotennantite-(Zn) from the Kvartsitoviye Gorki deposit, Kazahstan, was formally approved (Spiridonov et al., 1986), whereas Števko et al. (2018) had reported chemical data corresponding to argentotennantite-(Fe). Both minerals are characterized by the ideally fully occupied S(2) site, but no crystallographic data were available. Only recently were the first crystal chemical data on members of the arsenofreibergite series made available due to the description of kenoargentotennantite-(Fe) (Biagioni et al., 2026) and due to the present work, where argentotennantite-(Fe) is described. These data allow some comparison among these species (Table 8).

According to Spiridonov et al. (1986), the type material of argentotennantite-(Zn) has the chemical formula $(Ag_{5.67}Cu_{0.33})_{\Sigma 6.00}(Cu_{4.15}Zn_{1.52}Fe_{0.37}Pb_{0.01}Cd_{0.01})_{\Sigma 6.06}(As_{2.14}Sb_{1.89})_{\Sigma 4.03}S_{12.90}$, to be compared with its Fe analogue, whose chemical formula, as reported above, is $(Ag_{3.36}Cu_{2.70})_{\Sigma 6.06}(Cu_{4.05}Fe_{1.88}Zn_{0.07})_{\Sigma 6.00}(As_{2.29}Sb_{1.66})_{\Sigma 3.95}S_{12.82}$. The former has a higher Ag content, reflected in a larger unit-cell parameter, i.e., $a = 10.58$ Å, expanded with respect to that observed in argentotennantite-(Fe), $a = 10.44$ Å. In both species, a significant amount of Sb occurs, with As / (As + Sb) atomic ratios of 0.531 and 0.579 for the Zn and Fe isotypes, respectively. A non-negligible content of Sb also occurs in the keno-counterpart of argentotennantite-(Fe), i.e., kenoargentotennantite-(Fe), whose empirical for-

Table 8. Comparison of members of the arsenofreibergite series.

	Argentotennantite-(Fe)	Argentotennantite-(Zn)	Kenoargentotennantite-(Fe)
	[1]	[2]	[3]
End-member formula	$^{M(2)}Ag_6^{M(1)}(Cu_4Fe_2)$ $^{X(3)}As_4^{S(1)}S_{12}^{S(2)}S$	$^{M(2)}Ag_6^{M(1)}(Cu_4Zn_2)$ $^{X(3)}As_4^{S(1)}S_{12}^{S(2)}S$	$^{M(2)}Ag_6^{M(1)}(Cu_4Fe_2)$ $^{X(3)}As_4^{S(1)}S_{12}^{S(2)}\square$
$^{M(2)}Ag / (Ag + Cu)$	0.554	0.945	0.735
$^{M(1)}Fe / (Me^{2+})$	0.940	0.185	0.610
$^{X(1)}As / (Sb + As)$	0.580	0.531	0.702
$Y + Z$ (apfu)	12.82	12.90	12.12
a (Å)	10.4365(5)	10.584(3)	10.3740(5)
V (Å^3)	1136.75(17)	1185.6(6)	1116.45(16)
$M(2)$–S(1) (Å)	2.392	NA	2.445[a]/2.469[b]
$M(2)$–S(2) (Å)	2.242	NA	–[a]/2.24[b]
$M(1)$–S(1) (Å)	2.328	NA	2.334
U_{eq}S(2) (Å^2)	0.123	NA	0.046
VS(2)$_{oct.}$ (Å^3)	15.0	NA	12.1

$Me^{2+} = Zn + Fe + Cu^{2+} + Hg$. NA denotes not available. [a] Bond distance for $M(2a)$; [b] bond distance for $M(2b)$; [1] this paper; [2] Spiridonov et al. (1986); [3] Biagioni et al. (2026).

mula has been reported by Biagioni et al. (2026) as $(Ag_{4.41}Cu_{1.59})_{\Sigma 6.00}(Cu_{4.02}Fe_{1.22}Zn_{0.39}Hg_{0.37})_{\Sigma 6.00}(As_{2.80}Sb_{1.19})_{\Sigma 3.99}S_{12.12}\square_{0.88}$, with an As / (As + Sb) atomic ratio of 0.702. The presence of a significant amount of Sb in kenoargentotennantite-(Fe) has been interpreted considering the fact that, following Barton and Skinner (1978), the stability field of As_2S_3 is at a higher $f(S_2)$ than the Ag_2S–Ag equilibrium, and, consequently, As^{3+} could not coexist with Ag metal; on the contrary, below 300 °C, the equilibrium Sb_2S_3–Sb is below the Ag_2S–Ag equilibrium, suggesting that minor Sb seems necessary to stabilize kenoargentotennantite-(Fe). This hypothesis cannot be applied to argentotennantite-(Fe), where no hints of Ag–Ag bonding were observed. It is indeed possible that the occurrence of Sb is also necessary for steric reasons.

This is supported by some other natural occurrences of (Ag, As)-rich TGMs. For instance, Ixer and Stanley (1983) reported the chemistry of a grain of TGMs corresponding, on the basis of $\Sigma Me = 16$ apfu, to the composition (with rounding errors) $Ag_{6.02}(Ag_{1.91}Cu_{1.85}Zn_{1.44}Fe_{0.48}Cd_{0.16}Pb_{0.16})_{\Sigma 6.00}(As_{2.15}Sb_{1.87})_{\Sigma 4.02}S_{12.12}$ [As / (As + Sb) = 0.535], whereas Zakrzewski (1989) reported two chemical analyses corresponding to Fe- and Zn-rich members of the arsenofreibergite series with As / (As + Sb) atomic ratios of 0.500 and 0.502, respectively. In the zvěstovite series, the As / (As + Sb) ratio is 0.604 in zvěstovite-(Zn) (Sejkora et al., 2021) and 0.896 in zvěstovite-(Fe) (Biagioni et al., 2024).

As discussed by Johnson et al. (1988), the chemical composition of TGMs affects the framework rotation and the percent of distortion from ideality. In particular, the two most important parameters for the stability of TGMs are the size of the "spinner blades" (in the sense of Wuensch, 1964 – see Fig. 4 in his paper) and that of the $X(3)$ cations. The replacement of Cu by Ag at the $M(2)$ site increases both the rotation angle of the framework and its distortion. Figures 8 and 9 in Johnson et al. (1988) show that TGMs with $M(2)$ occupied by Ag and $X(3)$ hosting As show high values of both of these parameters, suggesting their instability owing to high structural strain. However, one can see that substituting As with Sb helps in reducing such a strain, thus allowing the existence of (Ag, As)-bearing TGMs. This is in line with Fig. 6b, which shows a negative correlation between the Ag content and the As / (As + Sb) ratio.

For this reason, even if the end-member formula of argentotennantite-(Fe) is defined to be $Ag_6(Cu_4Fe_2)As_4S_{13}$, its actual formula would be more correctly represented by the formula $Ag_6(Cu_4Fe_2)(As,Sb)_4S_{13}$.

4.4 Previous findings of argentotennantite-(Fe): a brief review

Tetrahedrite-group minerals with chemical compositions corresponding to that of argentotennantite-(Fe) were previously reported. To the best of our knowledge, the first chemical data corresponding to argentotennantite-(Fe) were reported by Števko et al. (2018) for part of the zoned TGM rims of argentotetrahedrite-(Zn) grains (Sejkora et al., 2022) from the Kremnica Au–Ag epithermal deposit, Slovakia. After recalculation of published chemical analyses (Števko et al., 2018) on the basis of $\Sigma Me = 16$ apfu, 11 spot analyses corresponded to argentotennantite-(Fe) with 3.02–3.77 apfu Ag, 1.31–1.98 apfu Fe, and S contents in the range of 12.54–12.99 apfu. Other parts of these rims are formed by kenoargentotennantite-(Fe), with 3.24–4.50 apfu

Ag and 11.70–12.49 apfu S (13 spot analyses), or Ag-rich tennantite-(Fe), with 0.67–2.99 apfu Ag (28 spot analyses). Later, Kolitsch et al. (2019) gave, for the Ag- and As-richest portions of zoned grains (10 µm in size) hosted in fluorite from the Grube Clara, Germany, the empirical formula $(Ag_{3.36}Cu_{2.64})Cu_4(Fe_{1.61}Zn_{0.39})(As,Sb)_4S_{13}$. Ondruš et al. (2003) published, for "argentotennantite" from Jáchymov, Czech Republic (grains up to 25 µm), contents of S in the range of 12.46–12.69 apfu, but after recalculation on the basis of $\Sigma Me = 16$ apfu, S contents were only 12.06–12.44 apfu, and so this phase may correspond to kenoargentotennantite-(Fe), with 3.17–4.29 apfu Ag and 1.52–1.84 apfu Fe.

5 Conclusions

Johnson et al. (1986) suggested the antipathetic relationship between Ag and As in TGMs, supported by some evidence regarding natural specimens collected between the 1970s and the 1980s (e.g., Charlat and Lévy, 1974; Wu and Petersen, 1977; Johnson and Burnham, 1985). However, other authors questioned this issue, supporting the existence of (Ag, As)-rich TGMs whose origin may be connected to P–T–X conditions (e.g., Foit and Ulbricht, 2001). As a matter of fact, up to recent times, no structural data on members of the arsenofreibergite series were available as the crystal structure of argentotennantite-(Zn) described by Spiridonov et al. (1986) was not refined.

The recent advancement in the knowledge of the crystal chemistry of TGMs allowed the collection of structural data on As analogues of the freibergite series, with the description of the new species kenoargentotennantite-(Fe) (Biagioni et al., 2026) and argentotennantite-(Fe). These species are further evidence of the plasticity of the crystal structure of TGMs, able to record the subtle variations of the ore geochemistry during the crystallization of these widespread sulfosalt minerals.

Data availability. The crystallographic information file data (CIF file) of argentotennantite-(Fe) and the full dataset of the chemical analyses of the described TGMs (Table S1) are available in the Supplement.

Supplement. The supplement related to this article is available online at https://doi.org/10.5194/ejm-38-325-2026-supplement.

Author contributions. JS, CB, and DV: conception of the project. JS, DV, and ZD: electron probe microanalysis and optical measurements. CB: single-crystal X-ray measurements and data interpretation. JS, JH, and CB: data interpretation and writing of the paper, with input from other authors.

Competing interests. At least one of the (co-)authors is a member of the editorial board of *European Journal of Mineralogy*. The peer-review process was guided by an independent editor, and the authors also have no other competing interests to declare.

Disclaimer. Publisher's note: Copernicus Publications remains neutral with regard to jurisdictional claims made in the text, published maps, institutional affiliations, or any other geographical representation in this paper. The authors bear the ultimate responsibility for providing appropriate place names. Views expressed in the text are those of the authors and do not necessarily reflect the views of the publisher.

Acknowledgements. We appreciate the many constructive comments of Tomáš Mikuš and Yves Moëlo, who helped us to improve this paper.

Financial support. The study was financially supported by the Ministry of Culture of the Czech Republic (long-term project DKRVO 2024-2028/1.II.c; National Museum, 00023272) and by Slovak Research and Development Agency (contract no. APVV-22-0041).

Review statement. This paper was edited by Sergey Krivovichev and reviewed by Tomáš Mikuš and Yves Moëlo.

References

Barton, P. B. and Skinner, B. J.: Sulfide mineral stabilities. In "Geochemistry of Hydrothermal Ore Deposits", 2nd edn., Holt, Rinehart et Winston, New York, 798 pp., 1978.

Biagioni, C., George, L. G., Cook, N. J., Makovicky, E., Moëlo, Y., Pasero, M., Sejkora, J., Stanley, C. J., Welch, M. D., and Bosi, F.: The tetrahedrite group: Nomenclature and classification, Am. Mineral., 105, 109–122, 2020.

Biagioni, C., Kasatkin, A. V., Nestola, F., Škoda, R., Gurzhiy, V. V., Agakhanov, A. A., and Koshlyakova, N. N.: Zvěstovite-(Fe), $Ag_6(Ag_4Fe_2)As_4S_{13}$, a new member of the tetrahedrite group from the Ulatayskoe Ag–Cu–Co occurrence, eastern Siberia, Russia, Eur. J. Mineral., 36, 529–540, https://doi.org/10.5194/ejm-36-529-2024, 2024.

Biagioni, C., Sejkora, J., Moëlo, Y., Makovicky, E., Musetti, S., Pasero, M., and Dolníček, Z.: Kenoargentotennantite-(Fe), $Ag_6(Cu_4Fe_2)As_4S_{12}\square$, a new "keno" member of the tetrahedrite group, Mineral. Mag., published online, 1–27, https://doi.org/10.1180/mgm.2026.10214, 2026.

Borčinová Radková, A., Jamieson, H., Lalinská-Voleková, B., Majzlan, J., Števko, M., and Chovan, M.: Mineralogical controls on antimony and arsenic mobility during tetrahedrite-tennantite weathering at historic mine sites Špania Dolina-Piesky and L'ubietová-Svätodušná, Slovakia, Am. Mineral. 102, 1091–1100, 2017.

Brese, N. E. and O'Keeffe, M.: Bond-valence parameters for solids, Acta Crystallogr., B47, 192–197, 1991.

Charlat, M. and Lévy, C.: Substitutions multiples dans la série tennantite-tétraédrite, Bull. Soc. fr. Minéral. Cristallogr., 97, 241–250, 1974.

Chetty, R., Bali, A., and Mallik, R. C.: Tetrahedrites as thermoelectric materials: an overview, J. Mater. Chem., C3, 12364–12378, 2015.

Criddle, A. J. and Stanley, C. J.: Quantitative data file for ore minerals, third edition, Chapman & Hall, London, ISBN 041246750X, 1993.

Crowley, J. A., Currier, R. H., and Szenics, T.: Mines and Minerals of Peru, 87–94: Huancavelica Group, Mineral. Rec., 28, 7–98, 1997.

D'Orazio, M., Biagioni, C., Fulignati, P., Gioncada, A., Sejkora, J., and Dolníček, Z.: Genesis and supergene weathering of tetrahedrite-(Hg) in meta-carbonate rocks: Bearing on differential mobility of priority pollutant metals, Ore Geol. Rev., 164, 105847, https://doi.org/10.1016/j.oregeorev.2023.105847, 2024.

Effenberger, H., Paar, W. H., Topa, D., Criddle, A. J., and Fleck, M.: The new mineral baumstarkite and a structural reinvestigation of aramayoite and miargyrite, Am. Mineral., 87, 753–764, 2002.

Flack, H. D.: On enantimorph-polarity estimation, Acta Crystallogr., A39, 876–881, 1983.

Foit Jr., F. F. and Ulbricht, M. E.: Compositional variation in mercurian tetrahedrite-tennantite from the epithermal deposits of the Steens and Pueblo Mountains, Harney County, Oregon, Can. Mineral., 39, 819–830, 2001.

Hyršl, J., Crowley, J. A., Currier, R. H., and Szenics, T.: Peru, paradise of minerals, Museum Andrés del Castillo, Lima, 1–543, 2010.

Ixer, R. A. and Stanley, C. J.: Silver mineralization at Sark's Hope mine, Sark, Channel Islands, Mineral. Mag., 47, 539–545, 1983.

Johnson, M. L. and Burnham, C. W.: Crystal structure refinement of an arsenic-bearing argentian tetrahedrite, Am. Mineral., 70, 165–170, 1985.

Johnson, N. E., Craig, J. R., and Rimstidt, J. D.: Compositional trends in tetrahedrite, Can. Mineral., 24, 385–397, 1986.

Johnson, N. E., Craig, J. R., and Rimstidt, J. D.: Effect of substitutions on the cell dimension of tetrahedrite, Can. Mineral., 25, 237–244, 1987.

Johnson, N. E., Craig, J. R., and Rimstidt, J. D.: Crystal chemistry of tetrahedrite, Am. Mineral., 73, 389–397, 1988.

Keim, M. F., Staude, S., Marquardt, K., Bachmann, K., Opitz, J., and Markl, G.: Weathering of Bi-bearing tennantite, Chem. Geol., 499, 1–25, 2018.

Keith, L. H. and Telliard, W. A.: Priority pollutants-I. A perspective view, Environ. Sci. Technol., 13, 416–423, 1979.

Kemkin, I. V. and Kemkina, R. A.: Microheterogeneity of the Koupol deposit fahlores as a reflection of changing of physicochemical parameters of the ore-forming solution, J. Earth Sci. 24, 179–187, 2013.

Kenngott, G. A.: Das Mohs'sche Mineralsystem, dem gegenwärtigen Standpuncte der Wissenschaft gemäss bearbeitet, Wien, 1853.

Kolitsch, U., Bayerl, R., and Topa, D.: Neufunde aus der Grube Clara im mittleren Schwarzwald (V), Mineralien-Welt, 30, 12–27, 2019.

Kovalenker, V. A. and Bortnikov, N. S.: Chemical composition and mineral association of sulphosalts in the precious metal deposits from different geological environment, Geol. Carpath., 36, 283–291, 1985.

Kraus, W. and Nolze, G.: POWDER CELL – a program for the representation and manipulation of crystal structures and calculation of the resulting X-ray powder patterns, J. Appl. Crystallogr., 29, 301–303, 1996.

Lewis Jr., R. W.: The geology, mineralogy and paragenesis of the Castrovirreyna lead-zinc-silver deposits, Peru (OFR No. 64-103), US Geological Survey, 1964.

Majzlan, J., Kiefer, S., Herrmann, J., Števko, M., Sejkora, J., Chovan, M., Lánczos, T., Lazarov, M., Gerdes, A., Langenhorst, F., Borčinová Radková, A., Jamieson, H., and Milovský, R.: Synergies in elemental mobility during weathering of tetrahedrite [$(Cu,Fe,Zn)_{12}(Sb,As)_4S_{13}$]: field observations, electron microscopy, isotopes of Cu, C, O, radiometric dating, and water geochemistry, Chem. Geol., 48, 1–20, 2018.

Mikuš, T., Vlasáč, J., Majzlan, J., Sejkora, J., Steciuk, G., Plášil, J., Rößler, C., and Matthes, C.: Argentotetrahedrite-(Cd), $Ag_6(Cu_4Cd_2)Sb_4S_{13}$, a new member of the tetrahedrite group from Rudno nad Hronom, Slovakia, Mineral. Mag., 87, 262–270, 2023.

Ondruš, P., Veselovský, F., Gabašová, A., Hloušek, J., Šrein, V., Vavřín, I., Skála, R., Sejkora, J., and Drábek, M.: Primary minerals of the Jáchymov ore district, J. Geosci., 48, 19–147, 2003.

Pažout, R., Dolníček, Z., Sejkora, J., and Štědrá, V.: Ag-Cu-Fe-Zn-Cd-As-Sb Mobilization in the Upper Part of the Oselské Pásmo Lode – An Unknown Story in the Evolution of Kutná Hora Ore District, Czech Republic, Minerals, 16, 196, https://doi.org/10.3390/min16020196, 2026.

Peterson, R. C. and Miller, I.: Crystal structure and cation distribution in freibergite and tetrahedrite, Mineral. Mag., 50, 717–721, 1986.

Pouchou, J. L. and Pichoir, F.: "PAP" ($\varphi\rho Z$) procedure for improved quantitative microanalysis, in: Microbeam Analysis, edited by: Armstrong, J. T., San Francisco Press, San Francisco, 104–106, 1985.

Qu, K., Sima, X., Gu, X., Sun, W., Fan, G., Yang, Z., and Wang, Y.: Kenoargentotetrahedrite-(Zn), $[Ag_6]^{4+}(Cu_4Zn_2)Sb_4S_{12}\square$, a new member of the tetrahedrite group from the Yindongpo Au deposit, China, Eur. J. Mineral., 36, 397–409, https://doi.org/10.5194/ejm-36-397-2024, 2024.

Rout, U., Tippireddy, S., Kumari, N., Dasgupta, T., and Mallik, R. C.: Effect of Ag-addition on the thermoelectric properties of $Cu_{12}Sb_4S_{13}$ tetrahedrite, J. Appl. Phys., 134, https://doi.org/10.1063/5.0184270, 2023.

Sejkora, J., Biagioni, C., Vrtiška, L., and Moëlo, Y.: Zvěstovite-(Zn), $Ag_6(Ag_4Zn_2)As_4S_{13}$, a new tetrahedrite-group mineral from Zvěstov, Czech Republic, Mineral. Mag., 85, 716–724, 2021.

Sejkora, J., Biagioni, C., Števko, M., Raber, T., Roth, P., and Vrtiška, L.: Argentotetrahedrite-(Zn), $Ag_6(Cu_4Zn_2)Sb_4S_{13}$, a new member of the tetrahedrite group, Mineral, Mag., 86, 319–330, 2022.

Sheldrick, G. M.: Crystal structure refinement with SHELXL, Acta Crystallogr., C71, 3–8, 2015.

Šoster, A., Zaccarini, F., and Zavašnik, J.: Tetrahedrite-(Hg) from the Litija deposit, Central Slovenia: Mineral chemistry insights into fluid evolution processes, Ore Geol. Rev., 173, 106272, https://doi.org/10.1016/j.oregeorev.2024.106272, 2024.

Spiridonov, E. M., Sokolova, N. G., Gapeev, A. K., Dashevskaya, D. M., Evstigneeva, T. L., Chvileva, T. N., Demidov, V. G., Balashov, E. P., and Shulga, V. I.: A new mineral – argentotennantite, Dokl. Akad. Nauk SSSR, 290, 206–210, 1986 (in Russian).

Staude, S., Mordhorst, T., Neumann, R., Prebeck, W., and Markl, G.: Compositional variation of the tennantite-tetrahedrite solid-solution series in the Schwarzwald ore district (SW Germany): the role of mineralization processes and fluid source, Mineral. Mag., 74, 309–339, 2010.

Števko, M., Sejkora, J., Dolníček, Z., and Škácha, P.: Selenium-rich Ag-Au mineralization at the Kremnica Au-Ag epithermal deposit, Slovak Republic, Minerals, 8, 572, https://doi.org/10.3390/min8120572, 2018.

Sun, F. H., Li, H., Tan, J., Zhao, L., Wang, X., Hu, H., Wang C., and Mori, T.: Review of current ZT > 1 thermoelectric sulfides, J. Materiomics, 10, 218–233, 2024.

Topa, D., Keutsch, F. N., and Stanley, C.: Sangenaroite, IMA 2019-014. CNMNC Newsletter No. 50, Mineral. Mag., 83, 617, https://doi.org/10.1180/mgm.2019.46, 2019.

Velebil, D., Hyršl, J., Sejkora, J., and Dolníček, Z.: Chemistry and classification of minerals of tetrahedrite group from deposits of Peru, Bull. Mineral. Petrolog., 29, 321–336, 2021 (in Czech).

von Weissenbach, C. G. A.: Ueber die Gehalte der beym sächsischen Bergbau vorkommenden Silbererze, Kalender für den Sächsischen Berg- und Hüttenmann auf das Jahr 1831, 223–248, 1831.

Wei, D., Xia, Y., Steadman, J. A., Xie, Z., Liu, X., Tan, Q., and Bai, L.: Tennantite-tetrahedrite-series minerals and related pyrite in the Nibao Carlin-type gold deposit, Guizhou SW China, Minerals, 11, 2, https://doi.org/10.3390/min11010002, 2021.

Welch, M. D., Stanley, C. J., Spratt, J., and Mills, S. J. Rozhdestvenskayaite $Ag_{10}Zn_2Sb_4S_{13}$ and argentotetrahedrite $Ag_6Cu_4(Fe^{2+},Zn)_2Sb_4S_{13}$: two Ag-dominant members of the tetrahedrite group, Eur. J. Mineral, 30, 1163–1172, 2018.

Weller, D. P. and Morelli, D. T.: Tetrahedrite thermoelectrics: from fundamental science to facile synthesis, Front. Electron. Mater., 2, 913280, https://doi.org/10.3389/femat.2022.913280, 2022.

Wilson, A. J. C. (Ed.): International Tables for Crystallography Volume C: Mathematical, Physical and Chemical Tables, Kluwer Academic Publishers, Dordrecht, the Netherlands, 1992.

Wise, J. M.: Undulatory silver-rich polymetallic veins of the Castrovirreyna district, central Peru: fault growth and mineralization in a perturbed local stress field, Econ. Geol., 100, 689–705, 2005.

Wu, I. and Petersen, U.: Geochemistry of tetrahedrite and mineral zoning at Casapalca, Peru, Econ. Geol., 72, 993–1016, 1977.

Wu, P., Yang,H., Qu K., Wang Y., and Gu X.: Argentotetrahedrite-(Hg) $Ag_6(Cu_4Hg_2)Sb_4S_{13}$: a new tetrahedrite group mineral from the Dongping Hg-Ag deposit, Hunan Province, China, Acta Geol. Sin., 96, 418–425, 2022 (in Chinese).

Wuensch, B.J.: The crystal structure of tetrahedrite, $Cu_{12}Sb_4S_{13}$, Z. Kristallogr., 119, 437–453, 1964.

Zakrzewski, M. A.: Members of the freibergite–argentotennantite series and associated minerals from the Silvermines, County Tipperary, Ireland, Mineral. Mag., 53, 293–298, 1989.